Development of an Algorithm for Crane Sway Suppression

Yasuhiro Yamamoto[a] , Chunnan Wu[a], Hisashi Osumi [b] , Masayuki Yano [c] and Yusuke Hara [b]

[a]Sumitomo Heavy Industries, LTD, Technology Research Center
[b]Chuo University, Faculty of Science and Engineering
[c]Chuo University, Graduate School of Science and Engineering
E-mail: yasuhiro.yamamoto@shi-g.com, chunnan.wu@shi-g.com, osumi@mech.chuo-u.ac.jp

Abstract –

In this research, a sway suppression algorithm was developed for a crane operator support system. To evaluate the effect of sway suppression, a crane experiment testbed was manufactured. The crane testbed is designed by the crane dynamic model, and the swing motion, boom motion and load hoisting are driven by the electric motors. The validity of the dynamic model for a crane was verified by the testbed experiment. The algorithm for sway suppression is consisted of the open loop control based on the phase plane theory, and was implemented in the testbed. The effect of sway suppression was verified by the testbed, and the effectiveness of algorithm was confirmed.

Keywords –

Crane; Sway Suppression; Phase Plane; Model

1 Introduction

In recent years, the number of skilled operator has decreased and many demands for safety work in construction site has increased. Therefore, the automation and improving safety function of construction machinery has become an important subject. Especially, there are many danger in rotary crane operation because of many reasons such as its fall down, load's sway, and so on.

There are many researches about sway suppression control of the translation crane[1][2][3]. Because the translation crane moves two axis independently, the load's sway in two dimensional plane can be suppressed easily.

But considering about the rotary crane, since it controls the load by swing and boom motion, it is difficult to move like the translation crane and the centrifugal force works to the load, so the load's sway is difficult to suppress.

For sway suppression for the rotary crane, there are some researches[4][5][6]. However, implementing feedback system or complex control system in real machine has many problems in ensuring safety.

To solve these problems, we had proposed a simple algorithm based on open loop control for crane sway suppression only using swing motion, and also developed a crane experiment testbed to evaluate the effect of the algorithm. This crane testbed has three electric motors for swing motion, boom motion and load hoisting, and we confirmed the effect of the algorithm by using the crane testbed.

2 Sway suppression algorithm

2.1 Principal of the algorithm

There are many researches of translation crane with using open loop control based on a phase plane which describes state of vibration[7][8]. The concept of the phase plane is shown in Figure 1, where l is the wire length, g gravitational acceleration, and θ deflection angle.
The equation of motion is described as Equation (1). From solving Equation (1), the deflection angle and angular velocity are described as Equation (2) and (3), where A is a constant.

$$\theta'' = -\frac{g}{l}\theta = -\omega^2\theta \quad (1)$$

$$\theta = Acos(\omega t) \quad (2)$$

$$\theta'/\omega = -Acos(\omega t) \quad (3)$$

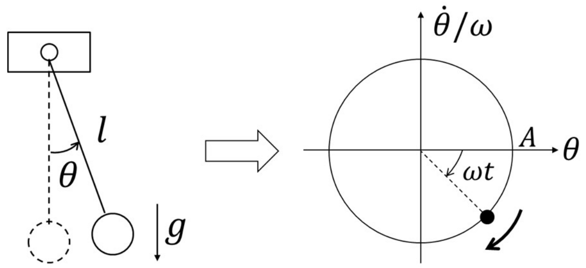

Figure 1. Concept of the phase plane

Based on Equation (2) and (3), the phase plane is described using the deflection angle as the horizontal axis, and the angular velocity, which normalized by natural frequency ω, as the vertical axis.

The motion of pendulum is translated as rotation motion in the phase plane, and the time required for one round is pendulum period T ($=2\pi/\omega$).

As shown in Figure 2, considering when the acceleration a is applied to the crane, the equation of motion changes to Equation (4). Transforming this equation into Equation (5), it can be seen the rotary motion on the phase plane is switched into the rotation which its center is $-a/g$.

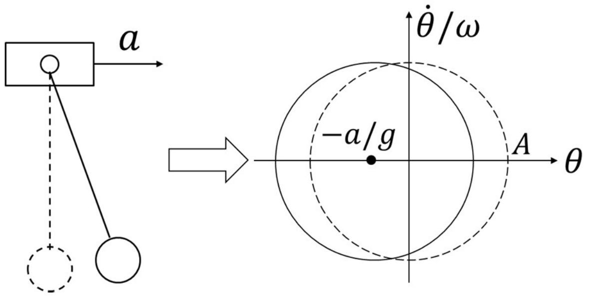

Figure 2. Effect of acceleration in the phase plane

$$\theta'' = -\frac{g}{l}\theta - \frac{1}{l}a \quad (4)$$

$$\left(\theta + \frac{a}{g}\right)'' = -\frac{g}{l}\left(\theta + \frac{a}{g}\right) \quad (5)$$

Hence, by giving the required acceleration at appropriate timing, the rotation motion can be directed to the origin. Shown in Figure 3, make the acceleration zero when the motion is reached to the origin, the vibration can be converged.

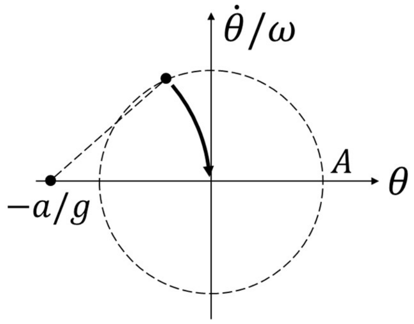

Figure 3. Convergence of the vibration

Based on the above theory, the acceleration pattern shown in Figure 4 is proposed as the sway suppression algorithm. According to this pattern, the acceleration a is first applied to the stopped crane for a time Δt. Next, the acceleration is set to zero for a time $T/2\text{-}\Delta t$, where the crane moves as uniform motion. Finally, setting the acceleration to a for a time Δt, the crane can accelerate without swaying. And then, after transporting the crane for arbitrary time, the crane can be stopped without swaying by applying the deceleration pattern, which the sign of the acceleration pattern is reversed.

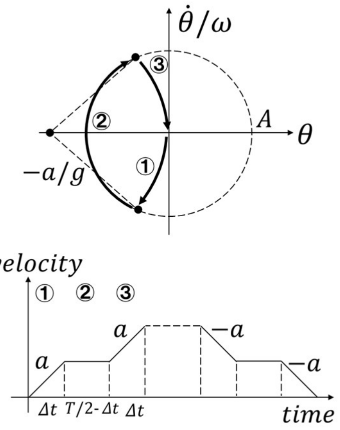

Figure 4. Sway suppression algorithm pattern

2.2 Pendulum model in crane's 3D motion

In order to apply the sway suppression pattern, which described in previous section, the dynamic model of the crane is expressed in this section. Figure 5 shows the model of the crane. By taking the coordinate system as shown in Figure 5, the position of boom tip (x, y, z) is expressed by Equation (4)~(6), where l is the wire length, g gravitational acceleration, B boom length, p swing angle, q boom angle, and ψ, φ sway angle.

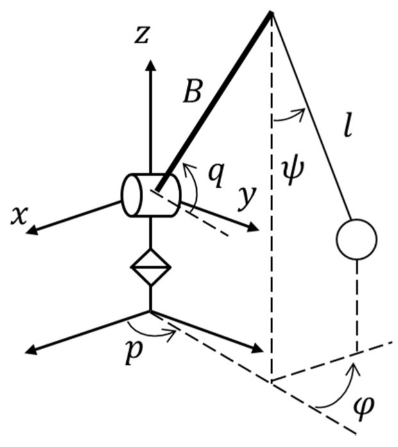

Figure 5. Crane dynamic model

$$x = B\cos q\cos p \quad (6)$$

$$y = B\cos q\sin p \quad (7)$$

$$z = B\sin q \quad (8)$$

Hence, the acceleration at the boom tip is described as Equation (9)~(11).

$$x'' = -Bq''\sin q\cos p - Bp''\cos q\sin p - B(q'^2 + p'^2)\cos q\cos p + 2Bq'p'\sin q\sin p \quad (9)$$

$$y'' = -Bq''\sin q\sin p + Bp''\cos q\cos p - B(q'^2 + p'^2)\cos q\sin p - 2Bq'p'\sin q\cos p \quad (10)$$

$$z'' = Bq''\cos q - Bq'^2\sin q \quad (11)$$

Then the position of load's centroid (x_p,y_p,z_p) can be described as Equation (12)~(14), where the origin of load's coordinate system is the boom tip.

$$x_p = l sin\psi cos\varphi \quad (12)$$

$$y_p = l sin\psi sin\varphi \quad (13)$$

$$z_p = -l cos\psi \quad (14)$$

According to Equation (12)~(14), the equations of rotary motion about ψ, φ are described as Equation (15), (16), where x'', y'', z'' is the acceleration at the boom tip described in Equation (9)~(11).

$$\psi'' = -\frac{1}{l}(2l'\psi' - l\varphi'^2 sin\psi cos\psi + g sin\psi + cos\psi cos\phi x'' + cos\psi sin\phi y'' + sin\psi z'') \quad (15)$$

$$\varphi'' = -\frac{1}{l sin\psi}(2l'\varphi' sin\psi + 2l\varphi'\psi' cos\psi - sin\varphi x'' + cos\varphi y'') \quad (16)$$

3 Simulation with crane testbed

3.1 Configuration of crane testbed

In the previous chapters, the sway suppression algorithm and the crane dynamic model were described.

In order to confirm these above, a crane experiment testbed has been made as shown in Figure 6.

Table 1 shows the specifications. The crane testbed has three electric motors for swing, boom and hoisting, and these motors has the encoder for measuring a motor angle and angular velocity. For holding the posture, the boom and hoisting motors are connected to the winches driven by the worm wheels.

Table 1. Specification of a crane experiment testbed

	Specification
Boom	length 1.0 m (parallel link)
Load	400.0 g (30.0*50.0*80.0mm)
Swing Motor	Max angular velocity 135.0 deg/s
Boom Motor	Max angular velocity 6.8 deg/s
Hoist Motor	Max angular velocity 32.6 deg/s
Camera	DFK Z30GP031 (30 fps)

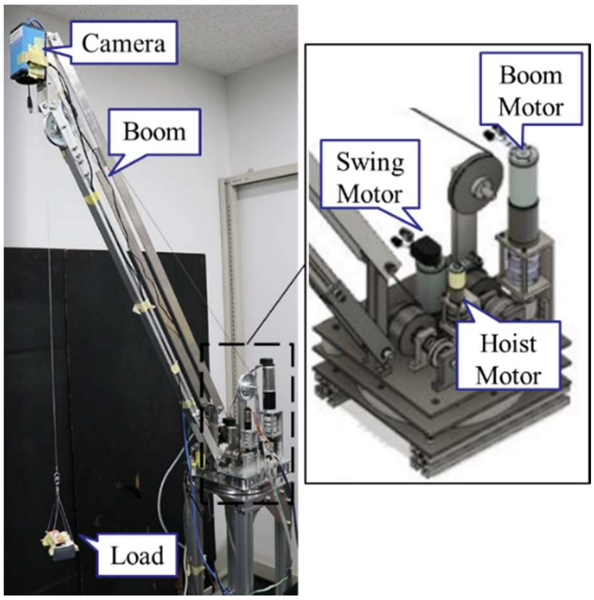

Figure 6. Crane experiment testbed

Here, a camera is mounted on the boom tip to measure the centroid of the load. The boom is composed of the parallel link so that the camera faces perpendicular downward regardless of the boom angle. Figure 7 shows the relationship of the coordinate of system between crane and camera. The *xy* coordinates of the camera (x_{cam}, y_{cam}) are expressed as a state, which they are rotated by $-\pi/2$ [rad] about *z* axis of the coordinate of crane and further by swing angle *p*.

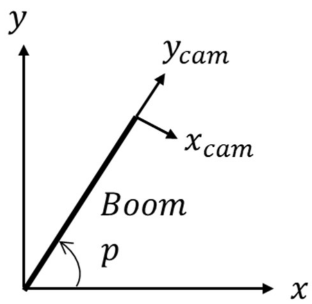

Figure 7. Camera coordinates

3.2 Configuration of control system

The control system configuration of the crane testbed is shown in Figure 8. This system has the crane testbed, a motor driver, an image processing PC for camera, a rapid controller which includes the crane dynamic model, and host PC for the rapid controller. These components are coupled and make one simulation system. The dynamic model in the rapid controller has been modelled as mathematical equations and implemented in MATLAB & SIMULINK models. The crane testbed is

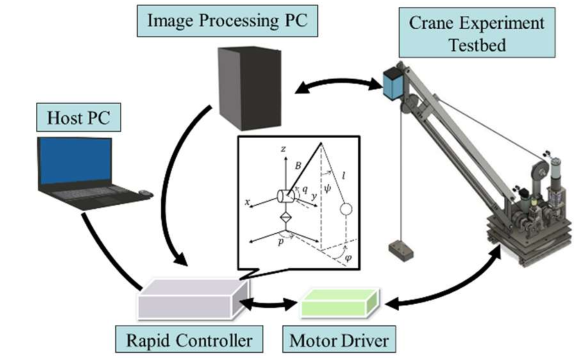

Figure 8. System Configuration

driven by the control signal, which outputted from the host PC via the rapid controller and the motor driver. In addition, the image acquired by the camera is sent to the image processing PC, and the *xy* coordinates of the load's centroid are calculated.

The *xy* coordinates are sent to the rapid controller for recording. The frame rate of the camera is 30 fps, and it is possible to calculate and output the coordinates of each frame in real time.

3.3 Verification of sway suppression

The sway suppression algorithm is verified in the crane testbed by applying the algorithm to the swing motor. The simulation conditions are shown in Table 2.

Table 2. Simulation conditions

	Specification
Wire	1 m fixed
Boom Angle	60 deg fixed
Swing Angle	90 deg swing
Transport time	5 s

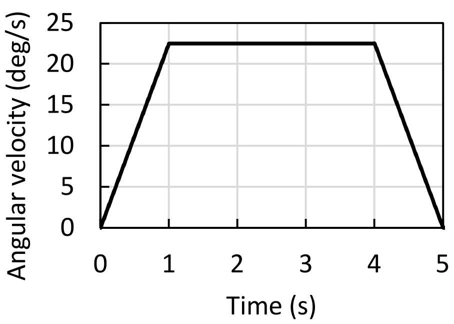

(a) Velocity Pattern

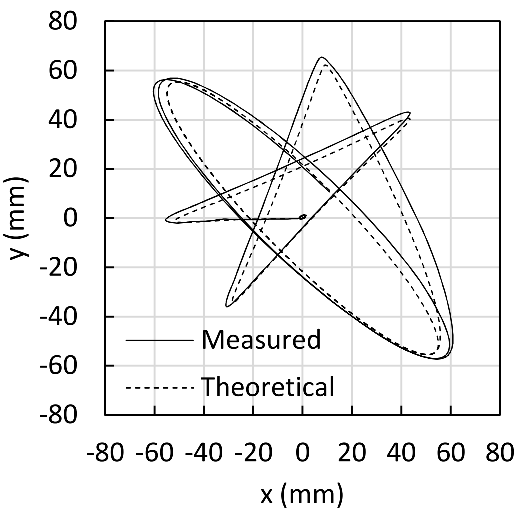

(b) Locus of load’s centroid

Figure 9. Experiment results

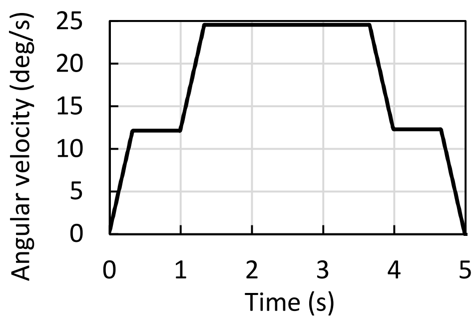

(a) Velocity Pattern

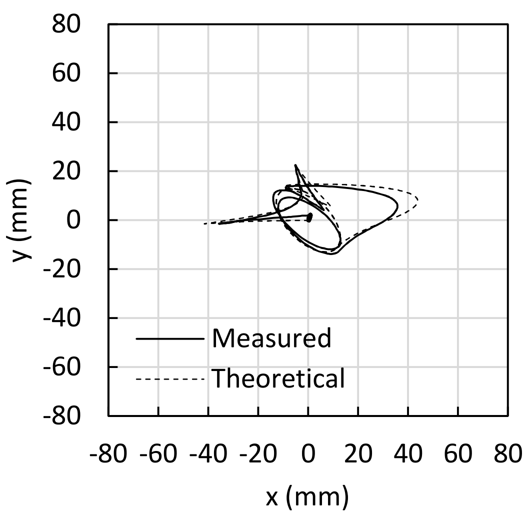

(b) Locus of load’s centroid

Figure 10. Experiment results

First, it is confirmed whether the behaviour of the load of the crane testbed follows the crane dynamic model. The results of the experiment are shown in Figure 9. The velocity pattern described in Figure 9 (a) is inputted to the swing motor, and then the locus of the load's centroid is observed, as shown in Figure 9 (b), by the camera on the boom tip.

Since this input pattern is not match the sway suppression algorithm pattern, it can be seen from the locus that the amplitude of the residual vibration ±60mm in the x direction and ±60mm in the y direction.

By comparing the locus calculated by the equation of motion with the measured locus of the load, the crane dynamic model is considered to be sufficient, though there are slight error in the locus. This error is considered to be occurred since there are many parameters not included in the equation of motion such as the vibration, expansion and contraction of the wire.

Next, the results of the experiment are shown in Figure 10 with inputting the sway suppression algorithm. The input pattern described in Figure 10(a) is inputted to the swing motor of the crane testbed, and then the locus of the load's centroid is observed, as shown in Figure 10(b).

Comparing with the result in Figure 9 (b), the amplitude of the residual vibration in Figure 10(b) is suppressed well, where the amplitudes are ±13mm in the x direction and ±13mm in the y direction. This residual vibration is mainly caused by the centrifugal force.

According to this experiment, the algorithm is also effective when it is applied only to the swing axis, if the posture change of crane is small during the acceleration and deceleration period.

Future work will aim the development of the sway suppression algorithm which includes the compensation of the centrifugal force, using this simulation system.

4 Conclusion

In this research, an algorithm for the crane sway suppression was proposed, which based on the phase plane theory, and confirmed its effectiveness by applying to a crane experiment testbed, which composed of the electrical motors and the link mechanism. And also, the validity of the crane dynamic model was verified.

According to the experimental results, it is confirmed that applying the algorithm only to the swing axis is effective, when the posture change of crane is small during the acceleration and deceleration period.

In future work, the new sway suppression algorithm needs to be proposed, which includes the compensation of the centrifugal force by the swing motion, and verified by applying to the crane testbed.

References

[1] Sun, You-Gang, et al. "The nonlinear dynamics and anti-sway tracking control for offshore container crane on a mobile harbor." Journal of Marine Science and Technology-Taiwan 25.6 (2017): 656-665.

[2] Chwa, Dongkyoung. "Sliding-mode-control-based robust finite-time antisway tracking control of 3-D overhead cranes." IEEE Transactions on Industrial Electronics 64.8 (2017): 6775-6784.

[3] Ahmad, Mohd Ashraf, and Zaharuddin Mohamed. "Hybrid Fuzzy Logic Control with Input Shaping for Input Tracking and Sway Suppression of a Gantry Crane System 1." (2009).

[4] Shen, Ying, and Kazuhiko Terashima. "Optimal control of rotary crane using the straight transfer transformation method to eliminate residual vibration." *Transactions of the Society of Instrument and Control Engineers* 39.9 (2003): 817-826.

[5] Ouyang, Huimin, Naoki Uchiyama, and Shigenori Sano. "S-curve trajectory generation for residual load sway suppression in a rotary crane system using only horizontal boom motion." *Journal of System Design and Dynamics* 5.7 (2011): 1418-1432.

[6] Ichise, Kenji, Shigeto Ouchi, and Kang Zhi Liu. "ANTI-SWAY CONTROL SYSTEM OF A ROTATIONAL CRANE USING A NON-LINEAR CONTROLLER." *The Proceedings of the International Conference on Motion and Vibration Control 6.2*. The Japan Society of Mechanical Engineers, 2002.

[7] Kobayashi, K., Y. Kato, and S. Nakano. "Development of an Automatic Operation System of Overhead Travelling Cranes in Steel Coil Warehouse." *IFAC Proceedings Volumes* 22.11 (1989): 311-315.

[8] Yamagishi, T. "Optimal control of load swing of crane." *IFAC Proceedings Volumes* 7.2 (1974): 345-355.